



HAL
open science

Alcohol Oxidation Assisted by Molybdenum Hydrazonato Catalysts Employing Hydroperoxide Oxidants

Josipa Mihalinec, Matea Pajski, Pascal Guillo, Mirna Mandarić, Nikol Bebić,
Jana Pisk, Višnja Vrdoljak

► **To cite this version:**

Josipa Mihalinec, Matea Pajski, Pascal Guillo, Mirna Mandarić, Nikol Bebić, et al.. Alcohol Oxidation Assisted by Molybdenum Hydrazonato Catalysts Employing Hydroperoxide Oxidants. *Catalysts*, 2021, 11 (8), pp.881. 10.3390/catal11080881 . hal-04808288

HAL Id: hal-04808288

<https://hal.science/hal-04808288v1>

Submitted on 28 Nov 2024

HAL is a multi-disciplinary open access archive for the deposit and dissemination of scientific research documents, whether they are published or not. The documents may come from teaching and research institutions in France or abroad, or from public or private research centers.



L'archive ouverte pluridisciplinaire **HAL**, est destinée au dépôt et à la diffusion de documents scientifiques de niveau recherche, publiés ou non, émanant des établissements d'enseignement et de recherche français ou étrangers, des laboratoires publics ou privés.



Distributed under a Creative Commons Attribution 4.0 International License

Article

Alcohol Oxidation Assisted by Molybdenum Hydrazonato Catalysts Employing Hydroperoxide Oxidants

Josipa Mihalinec¹, Matea Pajski¹, Pascal Guillo^{2,3} , Mirna Mandarić¹, Nikol Bebić¹, Jana Pisk^{1,*} 
and Višnja Vrdoljak^{1,*}

¹ Department of Chemistry, Faculty of Science, University of Zagreb, Horvatovac 102a, 10000 Zagreb, Croatia; josipa.mihalinec@chem.pmf.hr (J.M.); matea.pajski@chem.pmf.hr (M.P.); mirna.mandarić@chem.pmf.hr (M.M.); nikol.bebic@chem.pmf.hr (N.B.)

² Department of Chemistry, Institut Universitaire de Technologie Paul Sabatier, University of Toulouse, Av. G. Pompidou, BP20258, CEDEX, F-81104 Castres, France; pascal.guillo@iut-tlse3.fr

³ LCC-CNRS, Université de Toulouse, CNRS, UPS, CEDEX 4, F-31077 Toulouse, France

* Correspondence: jana.pisk@chem.pmf.hr (J.P.); visnja@chem.pmf.hr (V.V.); Tel.: +385-1-4606-350 (J.P.); +385-1-4606-353 (V.V.)

Abstract: Molybdenum(VI) catalysts were obtained from methanol or acetonitrile by the reaction of $[\text{MoO}_2(\text{C}_5\text{H}_7\text{O}_2)_2]$ and isonicotinoyl- or nicotinoyl-based aroylhydrazones. Reactions in methanol resulted in the formation of the mononuclear complexes $[\text{MoO}_2(\text{L}^{1-4})(\text{MeOH})]$ (**1a–4a**), while the ones in acetonitrile provided polynuclear complexes $[\text{MoO}_2(\text{L}^{1-4})]_n$ (**1–4**). Crystals of polynuclear compound, $[\text{MoO}_2(\text{L}^3)]_n \cdot \text{H}_2\text{O}$ (**3·H₂O**), suitable for X-ray diffraction analysis were obtained by the solvothermal procedure at 110 °C. Complexes were characterized by infrared spectroscopy (IR-ATR), nuclear magnetic resonance (NMR), elemental analysis (EA), and thermogravimetric analysis (TGA). The prepared catalysts were tested in alcohol oxidation reactions. Carveol, cyclohexanol, and butan-2-ol were investigated substrates. Because the alcohol oxidations are very challenging due to various possible pathways, the idea was to test different oxidants, H_2O_2 , TBHP in water and decane, to optimize the researched catalytic system.

Keywords: molybdenum; aroylhydrazone; alcohol oxidation; catalysis; organic solvent-free process; TBHP in decane; TBHP in water; H_2O_2



Citation: Mihalinec, J.; Pajski, M.; Guillo, P.; Mandarić, M.; Bebić, N.; Pisk, J.; Vrdoljak, V. Alcohol Oxidation Assisted by Molybdenum Hydrazonato Catalysts Employing Hydroperoxide Oxidants. *Catalysts* **2021**, *11*, 881. <https://doi.org/10.3390/catal11080881>

Academic Editor: Carla D. Nunes

Received: 30 June 2021

Accepted: 19 July 2021

Published: 22 July 2021

Publisher's Note: MDPI stays neutral with regard to jurisdictional claims in published maps and institutional affiliations.



Copyright: © 2021 by the authors. Licensee MDPI, Basel, Switzerland. This article is an open access article distributed under the terms and conditions of the Creative Commons Attribution (CC BY) license (<https://creativecommons.org/licenses/by/4.0/>).

1. Introduction

Catalytic oxidations of alcohols to corresponding aldehydes and ketones are of great importance and interest [1,2]. Since the usual oxidation processes imply the use of KMnO_4 , CrO_3 , and halogenated solvents, which are often environmentally harmful, there is a definite need for developing more eco-friendlier and economically affordable catalytic procedures [3]. Hydrogen peroxide, H_2O_2 , is often recommended oxidizing agent in that regard. Another option is *tert*-butyl hydroperoxide (TBHP) due to its solubility and stability in organic solvents [4]. The by-product of the reaction, *tert*-butanol can be easily separated by distillation, converted into methyl *tert*-butyl ether, and employed as a gasoline additive.

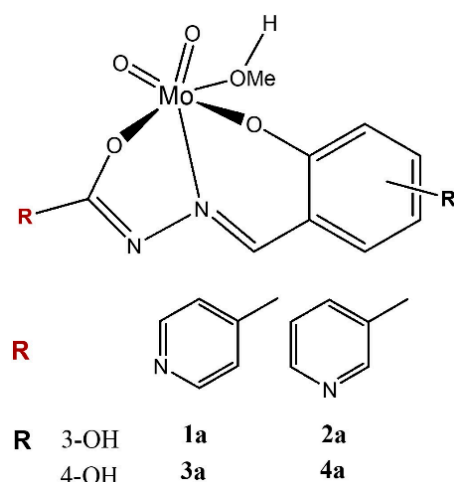
Typically, carveol is available as a mixture of *cis*- and *trans*- isomers [5]. *Trans*-carveol is an expensive ingredient of Valencia orange essential oil. The successful preparative method involved α -pinene oxide and zeolite catalyst [6]. The desired product, carvone takes place in the production of pharmaceuticals, fragrances, and flavours. It can be extracted from essential spearmint oils, but the great demand requires new chemical pathways for its production. For instance, it can be produced by the catalytic oxidation of limonene obtained from the orange peels. Literature reports carveol oxidation with hydrogen peroxide, $[\text{M}_4(\text{H}_2\text{O})_2(\text{PW}_9\text{O}_{34})_2]^{n-}$ ($\text{M} = \text{Co}^{\text{II}}, \text{Mn}^{\text{II}}, \text{Fe}^{\text{III}}, \text{Co}_4(\text{PW}_9)_2, \text{Mn}_4(\text{PW}_9)_2$, and $\text{Fe}_4(\text{PW}_9)_2$, respectively) as catalysts [7]. The conversion was almost complete, but the selectivity towards carvone was around 50%. Further, carveol oxidation with TBHP

over the phthalocyanine complex FePcCl_{16} immobilized on the mesoporous silica SBA-15, provided 75% of conversion and 40% selectivity towards carvone [8].

On the other hand, the majority of cyclohexanol and its mixtures are used as starting material in the synthesis of caprolactan and adipic acid, intermediates in the production of nylon. Not so far ago, direct production of adipic acid from cyclohexanone with oxygen or hydrogen peroxide was investigated [9,10]. Likewise, supported phosphotungstic acid on silica-coated MgAl_2O_4 nanoparticles with hydrogen peroxide showed great recovery possibilities for cyclohexanol oxidation [11], while selectivity towards the desired ketone with ruthenium pyridine-imine based complexes with N-methylmorpholine-N-oxide (NMO) was in the range 82–97% [12]. NMO showed great potential for selective oxidation of alcohols under mild conditions. The supreme problems of cyclohexanol oxidation rise within the steric effect of cyclohexyl group and competing reactions as aromatization to phenol, dehydration to cyclohexene, and condensation of cyclohexanone to cyclohexenyl cyclohexanone.

Dioxomolybdenum(VI) complexes with ONO ligands, prepared from 2,6-diformyl-4-methylphenol and hydrazides, used as catalysts and H_2O_2 , as an oxidant, showed good catalytic properties for 1-phenyl ethanol, propan-2-ol, and butan-2-ol oxidation [13]. CH_3CN was added to the reaction mixture for all the tested alcohols. The best results were obtained at 80 °C and by the addition of 5 mL CH_3CN . After 20 h, the alcohol conversions reached values 60–95%, and the ketone yields were 90–95%. Moreover, mononuclear molybdenum complexes with ligands obtained from 4-benzoyl-3-methyl-1-phenyl-2-pyrazoline-5-one and hydrazides, isonicotinoyl hydrazide, nicotinoyl hydrazide, 2-furoyl hydrazide and benzohydrazide, obtained from MeOH, were as well classified as good alcohol oxidation catalysts [14]. 1-phenylethanol, propan-2-ol and butan-2-ol were tested as substrates, H_2O_2 was an oxidant and CH_3CN was added to the reaction mixture, while complete reaction lasted 20 h. Furthermore, complexes of the formula $[\text{MoO}_2(\text{L})(\text{MeOH})]$ (L^{2-} derived from 4-[3,5-bis(2-hydroxyphenyl)-1,2,4-triazol-1-yl]benzoic acid or 3,5-bis(2-hydroxyphenyl)-1-phenyl-1,2,4-triazole), catalysed cyclohexanol oxidation with H_2O_2 as oxidant. In the presence of NEt_3 conversion of 50% was reached after 4 h, while without 20 h were needed [15]. Another interesting benzyl alcohol oxidation with Mo Schiff base complex supported on the Merrifield resin, with the assistance of H_2O_2 , and no addition of any organic solvents was presented [16]. The reaction lasted 2 h and isolated product yield was close to 100%.

In the present research, the main focus was on the carveol, cyclohexanol, and butan-2-ol oxidation reactions, with the assistance of molybdenum complexes containing aroylhydrazonato ligands (Scheme 1). Similar catalytic systems proved to be efficient catalysts for the cyclooctene epoxidation reactions and the aim was to extend the research to alcohol oxidations. Since the alcohol oxidations are very challenging due to different possible pathways leading to a wide class of by-products, the idea was to test different oxidants to optimize the catalytic system. For that reason, H_2O_2 , TBHP in water, and decane were chosen as oxidizing agents.



Scheme 1. The schematic presentation of the mononuclear $[\text{MoO}_2(\text{L}^{1-4})(\text{MeOH})]$ complexes coordinated with hydrazonate ligands bearing hydroxyl group **R**, at position 3 or 4.

2. Results and Discussion

2.1. Catalysts Preparation and Characterization

Syntheses of molybdenum(VI) catalysts were carried out in methanol and acetonitrile utilizing $[\text{MoO}_2(\text{C}_5\text{H}_7\text{O}_2)_2]$ and isonicotinoyl- ($\text{H}_2\text{L}^{1,3}$) or nicotinoyl-based hydrazones ($\text{H}_2\text{L}^{2,4}$). In all coordination compounds formed upon reaction, the ligands were coordinated to the $\{\text{MoO}_2\}^{2+}$ unit in the doubly deprotonated form L^{2-} (Scheme 1). Reactions in methanol resulted in the formation of the mononuclear complexes $[\text{MoO}_2(\text{L}^{1-4})(\text{MeOH})]$ (**1a–4a**), whereas those in acetonitrile gave polynuclear complexes $[\text{MoO}_2(\text{L}^1)]_n \cdot \text{MeCN}$ (**1**·MeCN) and $[\text{MoO}_2(\text{L}^{2-4})]_n$ (**2**, **3** and **4**). Crystals of $[\text{MoO}_2(\text{L}^3)]_n \cdot \text{H}_2\text{O}$ (**3**· H_2O) suitable for X-ray diffraction were obtained by the solvothermal procedure at 110 °C. The thermal analysis of the polynuclear complexes **1**·MeCN and **3**· H_2O , and single-crystal X-ray diffraction data for **3**· H_2O confirmed solvate formation. Complexes **1a–4a** transformed into polynuclear once after heating in acetonitrile.

Whereas the compound **1**·MeCN partially loses MeCN already upon standing at room temperature, crystals of **3**· H_2O are more stable and could be handled with less precaution. On the other hand, compounds **1a–4a** with coordinated solvent molecules are even more stable. According to the thermal analysis, they lose the coordinated MeOH in the range 178–210 °C (**1a**), 206–224 °C (**2a**), 120–175 °C (**3a**) and 214–247 °C (**4a**). Following decomposition, the final residue is MoO_3 .

In $[\text{MoO}_2(\text{L}^2)]_n \cdot \text{H}_2\text{O}$ (**3**· H_2O) the hydrazone coordinates the molybdenum atom of the *cis*- MoO_2^{2+} core tridentately through the phenolic and isonicotinoyl oxygens and azomethine-nitrogen (Figure 1a). The isonicotinoyl nitrogen atom of an adjacent complex unit occupies the remaining sixth coordination site thus enabling the formation of a one-dimensional polymer (Figure 1b). The distance Mo–N3 (2.427 Å) is the largest bond length within the molybdenum coordination sphere. According to the Cambridge Structural Database [17], only five Mo-coordination polymers with isonicotinoyl-based ligands were crystallized and structurally characterized so far [18–22]. The Mo–N bond in these structures has bond length in the range 2.426(6)–2.549(4) pm. The shortest one is in the polymer with 5-iodo-2-(olato)benzylidene)-(pyridine-4)carbohydrazone (Refcode GATGOA) [19] and the longest once in 4-(diethylamino)-2-(olato)benzylidene)-(pyridine-4)carbohydrazone (Refcode GELXUS) [17].

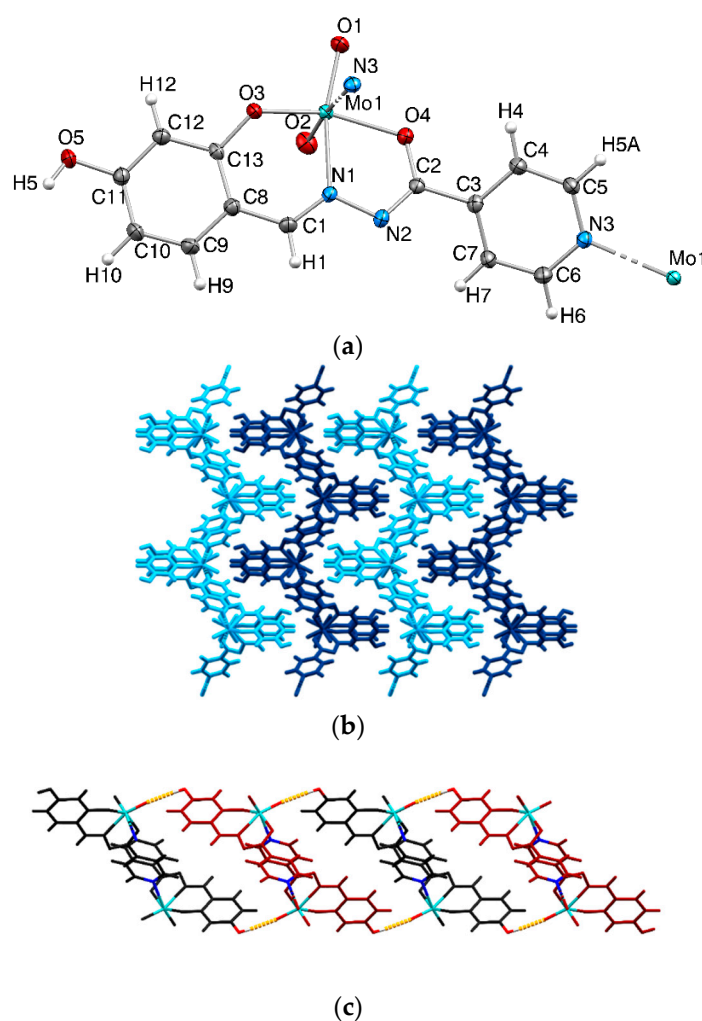


Figure 1. (a) ORTEP-PovRay plot of $3 \cdot \text{H}_2\text{O}$ with the atom-labelling scheme (displacement ellipsoids of non-hydrogen atoms are drawn at the 50% probability level, H_2O molecules are omitted for clarity). (b) Packing arrangement of the zigzag chains shown parallel to b -axis; (c) 1D chains are interconnected through hydrogen bonding interactions $\text{O5-H5} \cdots \text{O1}$.

As expected, the shortest bonds in polymer $3 \cdot \text{H}_2\text{O}$ are $\text{Mo}=\text{O1}$ and $\text{Mo}=\text{O2}$ (1.724(2) and 1.694(2) Å, respectively). Selected bond lengths and angles are given in Table S1, Supplementary Materials. In the complex the atoms are involved in hydrogen bonding $\text{O5-H5} \cdots \text{O1}$ (Figure 1c), and weak intermolecular hydrogen bonds $\text{C12-H12} \cdots \text{N2}$ and $\text{C1-H1} \cdots \text{O5}$, Table S2, Supplementary Materials.

The asymmetric and symmetric bands for $\{\text{MoO}_2\}$ core vibrations appear around $935\text{--}925\text{ cm}^{-1}$ in the IR spectra, and these bands tend to overlap. The interaction $\text{Mo}=\text{O}_t \cdots \text{Mo}$ in **1–4** is excluded due to the absence of broadband at $\sim 800\text{ cm}^{-1}$ in their spectra (Figure S1). Instead, a strong band belonging to $\nu(\text{O}=\text{Mo}-\text{N})$ around 900 cm^{-1} appears and is used to indicate the polymer formation. For the mononuclear complexes **1a–4a**, this band is replaced with a new one of differing intensity due to $\nu(\text{O}=\text{Mo}-\text{O}_{\text{MeOH}})$ stretching (Figure S2). Furthermore, a new band at $\sim 1020\text{ cm}^{-1}$ due to the $\text{C}-\text{O}_{\text{MeOH}}$ vibrations appears in the spectra. However, for polymer, no significant band is observed in that region. The band at $\sim 1340\text{ cm}^{-1}$, assigned to the $\text{C}-\text{O}$ group of the hydrazone moiety, and bands at $\sim 1600\text{ cm}^{-1}$ and 1250 cm^{-1} , belonging to $\text{C}=\text{N}_{\text{imine}}$ and $\text{C}-\text{O}_{\text{ph}}$ groups, respectively, indicate coordination of the ligand to the $\{\text{MoO}_2\}^{2+}$ unit through the ONO atoms of these three functional groups.

The coordination via *ONO* donor atoms is also maintained in the solution as confirmed by the NMR analysis (Tables S3 and S4, Figures S1 and S2, Supplementary Materials). The singlets belonging to the NH (=N–NH–(C=O)–) and OH-2' protons are absent in the ^1H NMR spectra of the complexes, indicating ligand tautomerization (to =N–N=(C–OH)–) and coordination through the deprotonated oxygen atoms. Significant deshielding of carbons adjacent to donor *ONO* atoms is observed, being larger for carbons at positions 1 and 4 (up to 8.01 ppm and 5.66 ppm, respectively) than for the carbon at position 2' (up to 2.04 ppm), Table 1, Scheme 1. Signals arising from free MeOH (ca. one equivalent), seen in the spectra of **1a–4a**, are suggesting MeOH co-ligand substitution with $\text{dms-}d_6$.

Table 1. The ^{13}C coordination chemical shifts $\Delta\delta(\text{ppm})$ for carbon atoms adjacent to *ONO* donors.

Complex	1	2	3	4
Atom	$\Delta\delta/\text{ppm}$			
C-1	8.01	7.56	7.26	6.9
C-4	5.66	5.65	4.47	4.44
C-2'	2.04	1.96	2.02	1.88

2.2. Catalytic Results

Oxidation of secondary alcohols carveol, cyclohexanol, and but-2-ol, catalysed by molybdenum(VI) complexes **1–4** and **1a–4a** was studied. The effects of various factors (i) oxidant: THBP (aqueous solution and in decane) vs. H_2O_2 , (ii) ligand: the influence of isonicotinic vs. nicotinic acid hydrazide and/or 2,3- vs. 2,4-dihydroxybenzaldehyde, (iii) type of complex (polynuclear vs. mononuclear) was investigated.

The reactions were carried out at 80 °C in a stirred solution of the substrate, catalyst, and oxidant in acetonitrile for 5 h. All the complexes were insoluble in acetonitrile at room temperature (orange slurry) but dissolved after 150 min in the carveol reaction mixture or after 20 min in the cyclohexanol reaction mixture at 80 °C (orange mixture turn yellow until the end of the reaction). The conversion of substrates was calculated according to an internal standard, acetophenone.

2.2.1. Carveol Oxidation

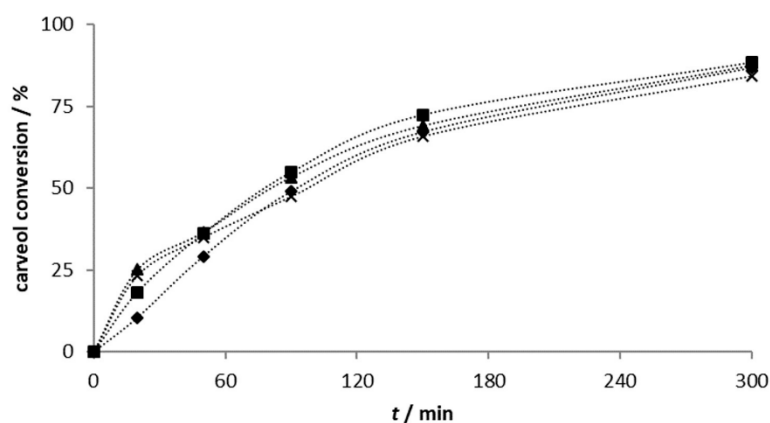
In order to find efficient and eco-friendlier catalytic system reactions were conducted with low Mo loading $n(\text{Mo}):n(\text{substrate}):n(\text{oxidant}) = 1:400:800$, where oxidant is H_2O_2 or THBP (solution in water or decane).

In the case of H_2O_2 , the conversion of carveol is high (84–91%) for all tested molybdenum complexes, following the order **4a** > **3a** > **1** > **2** = **1a** > **2a** > **4** > **3** (Table 2). All catalysts show similar values of selectivity towards carvone (41–44%). $\text{TOF}_{20\text{ min}}$ for the complexes obtained from 2,3-dihydroxybenzaldehyde (**1**, **2**, **1a**, **2a**) showed higher values in comparison to the complexes obtained from 2,4-dihydroxybenzaldehyde (**3**, **4**, **3a**, **4a**) implying faster activation time and conversion to the pentacoordinate active species $[\text{MoO}_2\text{L}]$. TON values for all the complexes, except **3** and **1a**, were up to 300. Since the oxidation system employing H_2O_2 and the complexes obtained from the ligands H_2L^1 and H_2L^2 showed better results in terms of tested catalytic parameters, further investigation was continued with the complexes **1**, **2**, **1a**, and **2a**. Kinetic profiles of polynuclear and mononuclear complexes were presented in Figure 2.

Table 2. Results of the carveol oxidation catalysed with molybdenum(VI) complexes under following conditions $n(\text{Mo}):n(\text{substrate}):n(\text{oxidant}) = 1:400:800$, $T = 353 \text{ K}$.

Catalyst	Conversion ^a /%	Selectivity ^b /%	TOF _{20 min} ^c /h ⁻¹	TON ^d
H ₂ O ₂				
1	88	41	113	308
2	87	42	294	339
3	77	40	4	30
4	85	44	34	329
1a	87	41	23	36
2a	84	41	286	344
3a	89	37	27	367
4a	91	42	20	394
THBP (in water)				
1	64	10	237	235
2	66	10	29	27
1a	62	11	29	27
2a	56	19	185	271
THBP (in decane)				
2a	99	4	1001	289

^a Carveol consumed at the end of reaction. ^b Formed carveone per converted olefin at the end of reaction. ^c $n(\text{carveol})$ transformed/ $n(\text{catalyst})$ /time(h) at 20 min. ^d $n(\text{carveol})$ transformed/ $n(\text{catalyst})$ at the end of reaction.

**Figure 2.** Converted carveol vs. time with molybdenum(VI) (pre)catalyst \blacklozenge complex **1**, \blacksquare complex **1a**, \blacktriangle complex **2**, \times complex **2a**. Conditions: $n(\text{Mo}):n(\text{substrate}):n(\text{H}_2\text{O}_2) = 1:400:800$, $T = 353 \text{ K}$.

On the other hand, for the tested molybdenum catalysts, **1**, **2**, **1a**, and **2a**, conversion of carveol with aqueous THBP was in the range 56 to 66%, with low selectivity towards carveone (10–19%). The kinetic profile was presented in Figure 3. Interestingly, complex **2a** with aqueous THBP showed the lowest carveol conversion (56%), but the highest selectivity towards carveone (19%) compared to other catalysts. It seems that a slower reaction rate seems to favour carveone formation. Additionally, the catalytic activity of the complex **2a** was tested in the presence of THBP solution in decane, and remarkable carveol conversion is achieved (99%) after 20 min of the reaction. It is not surprising that TOF_{20 min} achieved a value of 1001.

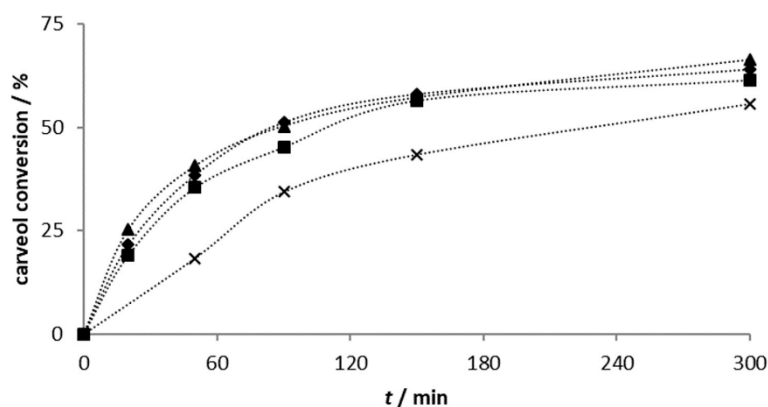


Figure 3. Converted carveol vs. time with molybdenum(VI) (pre)catalyst ♦ complex 1, ■ complex 1a, ▲ complex 2, × complex 2a. Conditions: $n(\text{Mo}):n(\text{substrate}):n(\text{THBP}_{\text{aq}}) = 1:400:800$, $T = 353 \text{ K}$.

However, due to low selectivity towards carveone (4%) (Table 2), further testing of other complexes was not performed under these conditions.

Since carveol contains two double bonds that may be targeted by the oxidant, relatively high conversion of carveol, accompanied by low selectivity towards carveone, can be expected. According to the literature, carveol epoxidation is the most likely to occur, which further explains low carveone yield (Figure 4) [23–25].

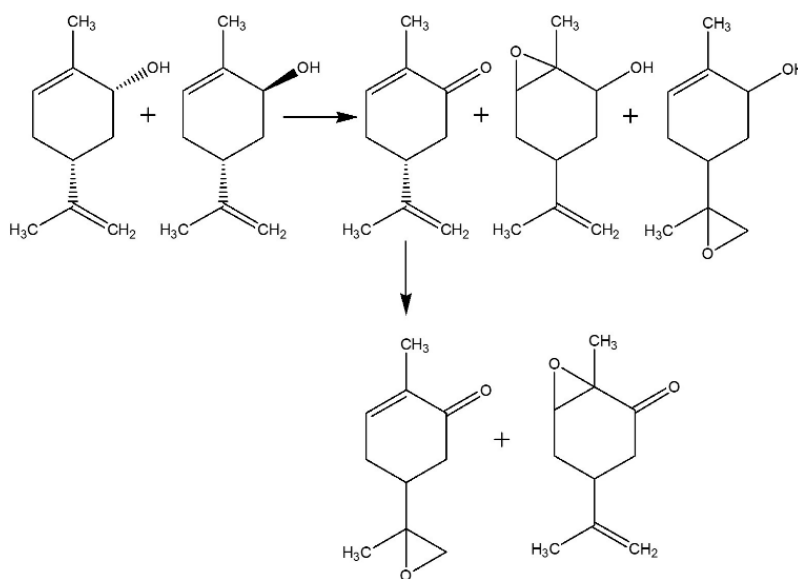


Figure 4. Oxidation scheme for carveol and carveone.

The obtained results imply that the substituent on the ligand (isonicotinic vs. nicotinic acid hydrazide) and type of complex (polynuclear vs. mononuclear) do not influence a lot on carveol oxidation. On the other hand, the effect of the used oxidant on the selectivity towards carveone should be discussed. During the reaction, a different consumption of *cis*- and *trans*- carveol was observed in the GC chromatogram for each of the oxidants. Having the latest in mind, different carveone selectivity can be explained by reaction stereoselectivity towards *cis*- or *trans*- carveol. By $^1\text{H-NMR}$ analysis [26] of the obtained reaction mixtures, it was seen that in the presence of H_2O_2 , the preferred substrate is *cis*-carveol, while with aqueous THBP, is *trans*-carveol (Figure 5).

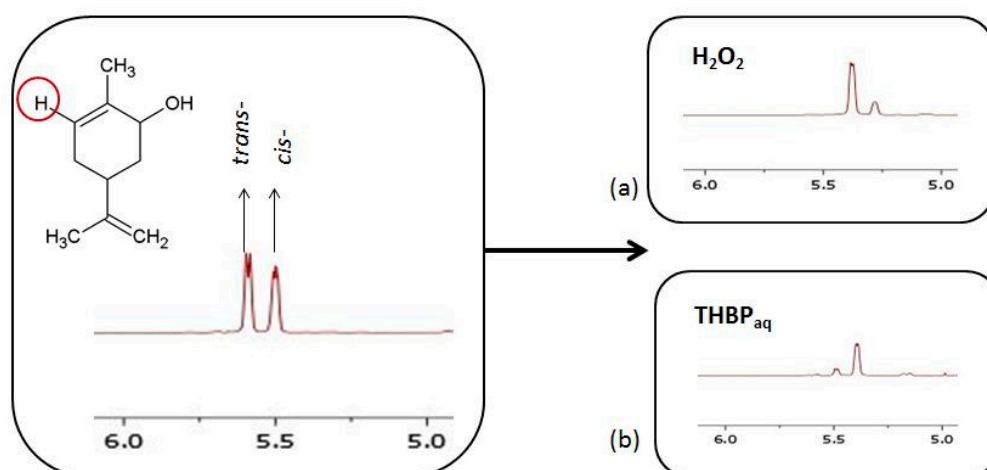


Figure 5. The extracted part of ^1H NMR spectra: (left) mixture of *cis*- and *trans*- carveol, reaction mixture with (a) H_2O_2 or (b) THBP_{aq} in the presence of complex **2**.

In addition, a high peak, belonging to the unknown compound **A**, could be detected in the GC chromatogram. In the reaction mixture with H_2O_2 , carveone was the main product and unknown compound **A** is a by-product. However, when using TBHP as an oxidant, unknown compound **A** was the main product. Further discussion in that regard is available in the Supplementary Materials.

2.2.2. Cyclohexanol Oxidation

At first, reactions were conducted with low Mo loading, ($n(\text{Mo}):n(\text{substrate}):n(\text{oxidant}) = 1:400:800$, where oxidant is H_2O_2 or THBP (in water or in decane), protocol A in the Experimental part. Since cyclohexanol conversion was extremely low in H_2O_2 , <10% for all the catalysts, the testing with other oxidants was continued only with the complexes **2a**. The cyclohexanol conversion is extremely low, 11% for **2** and 13% for **2a**, but selectivity towards cyclohexanol is moderate, 64% for **2** and 59% for **2a**.

All relevant catalytic data are presented in Table 3. A catalytic system with complex **2a** and THBP solution in the decane provides the highest cyclohexanol conversion (28%) and cyclohexanone yield (16%), while the selectivity towards cyclohexanone is the same as with H_2O_2 (59%). The use of TBHP in water did not result in better **2a** activity, and selectivity towards cyclohexanone was even diminished. However, the use of TBHP in decane provided better substrate conversion, 28%, while the cyclohexanone selectivity remained the same as with H_2O_2 .

Table 3. Results of the cyclohexanol oxidation catalysed with molybdenum(VI) complex **2** and **2a** in the presence of different oxidants after 5 h ($n(\text{Mo}):n(\text{substrate}):n(\text{oxidant}) = 1:400:800$, $T = 353$ K).

Catalyst	Oxidant	Conversion ^a /%	Selectivity ^b /%
2	H_2O_2	11	64
	H_2O_2	13	59
2a	THBP (in water)	17	31
	THBP (in decane)	28	59

[a] cyclohexanol consumed at the end of the reaction. [b] Formed ketone per converted alcohol at the end of the reaction.

Due to the very low results, higher catalyst loading, 1%, and lower content of oxidant was investigated (protocol B in the Experimental part), with H_2O_2 as an oxidant. All molybdenum(VI) complexes were tested within the following reaction conditions, $n(\text{Mo}):n(\text{substrate}):n(\text{H}_2\text{O}_2) = 1:100:300$. The results are summarized in Table 4.

Table 4. Results of the cyclohexanol oxidation catalysed with molybdenum(VI) complex in the presence of H₂O₂ after 5 h ($n(\text{Mo}):n(\text{substrate}):n(\text{oxidant}) = 1:100:300$, $T = 353 \text{ K}$).

Catalyst	Conversion ^a /%	Selectivity ^b /%	TOF _{20min} ^c /h ⁻¹	TON ^d
1	19	59	3	19
2	16	66	2	16
3	20	57	3	31
4	19	61	4	20
1a	21	66	4	21
2a	15	71	3	15
3a	14	68	76	14
4a	19	61	4	20

^a cyclohexanol consumed at the end of reaction. ^b Formed ketone per converted alcohol at the end of reaction. ^c $n(\text{cyclohexanol})$ transformed/ $n(\text{catalyst})$ /time(h) at 20 min. ^d $n(\text{cyclohexanol})$ transformed/ $n(\text{catalyst})$ at the end of reaction.

Slightly higher conversion for all the tested catalysts is achieved after 5 h (15–21%), followed by the higher values of selectivity towards cyclohexanone, the lowest being 57% for complex **3** and the highest one 71% for complex **2a**.

2.2.3. Butan-2-ol Oxidation

Considering that in our previous investigations, mononuclear complexes usually showed slightly better activity, catalysts **1a–4a** were tested for oxidation of butan-2-ol. Knowing the fact that MeCN provides better activity and selectivity towards the desired product, MeCN was added to both catalytic systems, containing H₂O₂ and aqueous TBHP. As seen from the results compiled in Table 5, MeCN did not have any tremendous effect on the tested reaction. In general, the selectivity towards butan-2-one is slightly better when MeCN is added and the catalyst is faster transferred into active species (concluded from TOF_{20 min} values). However, TON values remain similar, no matter the addition of the solvent. Furthermore, the nature of the used oxidant does not have a dramatic effect on the catalytic process.

Table 5. Results of the butan-2-ol oxidation catalysed with molybdenum(VI) complexes under conditions $n(\text{Mo}):n(\text{substrate}):n(\text{oxidant}) = 1:400:800$, $T = 353 \text{ K}$. $V(\text{MeCN}) = 2.5 \text{ mL}$.

Catalyst	Oxidant	Conversion ^a /%	Selectivity ^b /%	TOF _{20 min} ^c /h ⁻¹	TON ^d
1a	H ₂ O ₂	11	54	27	43
	H ₂ O ₂ + MeCN	12	57	31	49
	TBHP	17	45	99	52
	TBHP + MeCN	13	59	170	52
2a	H ₂ O ₂	23	40	44	90
	H ₂ O ₂ + MeCN	16	61	17	66
	TBHP	17	60	104	69
	TBHP + MeCN	37	57	117	151
3a	H ₂ O ₂	13	64	38	52
	H ₂ O ₂ + MeCN	13	69	30	52
	TBHP	19	51	83	73
	TBHP + MeCN	15	52	153	54
4a	H ₂ O ₂	14	49	71	55
	H ₂ O ₂ + MeCN	15	59	91	59
	TBHP	16	56	108	64
	TBHP + MeCN	14	47	26	56

^a butan-2-ol consumed at the end of reaction. ^b formed epoxide per converted olefin at the end of reaction. ^c $n(\text{butan-2-ol})$ transformed/ $n(\text{catalyst})$ /time(h) at 20 min. ^d $n(\text{butan-2-ol})$ transformed/ $n(\text{catalyst})$ at the end of reaction.

In comparison to the similar reported investigations with molybdenum Schiff base catalysts [13–15], the catalytic process presented within this research, provide great potential. For carveol oxidation, the system employing H_2O_2 provided to be the best one, justifying and following the principles of green processes. Cyclohexanol and butan-2-ol oxidation reactions, after 5 h, resulted with very good ketone yields, while the conversion parameter demands further optimization.

3. Materials and Methods

3.1. Preparative Part

All the starting compounds, aldehydes (Alpha-Aesar), and hydrazide (Alpha-Aesar, Germany), as well as all the substrates (Sigma-Aldrich, France) and oxidants, 30% H_2O_2 , 70% TBHPaq, 5.5 M TBHP in decane (Sigma-Aldrich, France) used for oxidation reaction, MeCN (Alpha-Aesar, Germany), and MeOH (Aldrich, France), were of reagent grade and used as purchased. The starting complex $[\text{MoO}_2(\text{acac})_2]$ (acac = acetylacetonate) [27], and hydrazones, were prepared as described in the literature [28].

3.1.1. Synthesis of the Polynuclear Molybdenum Complexes

A mixture of the starting complex $[\text{MoO}_2(\text{C}_5\text{H}_7\text{O}_2)_2]$ (0.032 g; 0.098 mmol) and the appropriate hydrazone H_2L^{1-4} (0.032 g; 0.098 mmol) in acetonitrile (40 mL) was refluxed for 3 h. The solution was left at room temperature for a few days, and the orange substance deposited was filtered, rinsed with acetonitrile, and dried. Crystals of $3 \cdot \text{H}_2\text{O}$ were obtained by the solvothermal procedure at 110 °C in a Teflon-lined stainless-steel autoclave upon addition of 10 μL of H_2O to the reaction mixture. (i) Anal. Calcd. for $\text{C}_{13}\text{H}_9\text{MoN}_3\text{O}_5$ ($M_r = 383.168$): C, 40.75; H, 2.37; N, 10.97%. TG: MoO_3 , 37.57%. (ii) Anal. Calcd. for MeCN solvate $\text{C}_{15}\text{H}_{12}\text{MoN}_4\text{O}_5$ ($M_r = 424.212$): TG: MeCN, 9.68; MoO_3 , 33.93%. (iii) Anal. Calcd. for H_2O solvate $\text{C}_{13}\text{H}_{11}\text{MoN}_3\text{O}_6$ ($M_r = 401.18$): H_2O , 4.5; MoO_3 , 35.88%.

$[\text{MoO}_2(\text{L}^1)]_n \cdot \text{MeCN}$ (**1**·MeCN): Yield 0.028 g (75%). The sample for elemental analysis was desolvated and analysed as **1**. Found: C 42.35, H 2.51, N, 13.00%. IR-ATR (cm^{-1}): 2249, 2160 ($\text{C}\equiv\text{N}$)_{MeCN}, 1605 ($\text{C}=\text{N}$), 1350 ($\text{C}-\text{O}_{\text{hyd}}$), 1233 ($\text{C}-\text{O}_{\text{ph}}$) 937, 925 ($\text{Mo}=\text{O}$), 908 ($\text{O}=\text{Mo}-\text{N}$). TG: CH_3CN , 9.37; MoO_3 , 34.51%.

$[\text{MoO}_2(\text{L}^3)]_n$ (**2**): Yield 0.028 g (75%). Found: C 41.41, H 2.11, N, 10.42%. IR-ATR (cm^{-1}): 1602 ($\text{C}=\text{N}$), 1343 ($\text{C}-\text{O}_{\text{hyd}}$), 1228 ($\text{C}-\text{O}_{\text{ph}}$), 937, 920 ($\text{Mo}=\text{O}$), 898 ($\text{O}=\text{Mo}-\text{N}$). TG: MoO_3 , 37.33%.

$[\text{MoO}_2(\text{L}^2)]_n$ (**3**): Yield 0.035 g (94%). Found: C 40.36, H 2.05, N, 40.55%. IR-ATR (cm^{-1}): 1601 ($\text{C}=\text{N}$), 1339 ($\text{C}-\text{O}_{\text{hyd}}$), 1231 ($\text{C}-\text{O}_{\text{ph}}$), 934, 915 ($\text{Mo}=\text{O}$), 895 ($\text{O}=\text{Mo}-\text{N}$). TG: MoO_3 , 38.02%

$[\text{MoO}_2(\text{L}^2)]_n \cdot \text{H}_2\text{O}$ (**3**· H_2O): 3233 (H_2O), 1599 ($\text{C}=\text{N}$), 1342 ($\text{C}-\text{O}_{\text{hyd}}$), 1233 ($\text{C}-\text{O}_{\text{ph}}$), 939, 914 ($\text{Mo}=\text{O}$), 885 ($\text{O}=\text{Mo}-\text{N}$). TG: H_2O , 4.11; MoO_3 , 36.50%.

$[\text{MoO}_2(\text{L}^4)]_n$ (**4**): Yield 0.030 g (81%). Found: C 40.67, H 2.07, N, 10.23%. IR-ATR (cm^{-1}): 1603 ($\text{C}=\text{N}$), 1327 ($\text{C}-\text{O}_{\text{hyd}}$), 1222 ($\text{C}-\text{O}_{\text{ph}}$) 935, 922 ($\text{Mo}=\text{O}$), 885 ($\text{O}=\text{Mo}-\text{N}$). TG: MoO_3 , 37.25%.

3.1.2. Synthesis of the Mononuclear Molybdenum Complexes

All complexes were prepared by heating $[\text{MoO}_2(\text{C}_5\text{H}_7\text{O}_2)_2]$ (0.1 g, 0.30 mmol) and the appropriate hydrazone H_2L^{1-4} (0.30 mmol) for 3.5 h in 30 mL methanol. The solution was left at room temperature for a few days and the obtained orange product was filtered, rinsed with methanol, and dried. Anal. Calcd., for $\text{C}_{14}\text{H}_{13}\text{MoN}_3\text{O}_6$ ($M_r = 415.209$): C 40.50; H 3.16; N 10.12%. TG: CH_3OH , 7.72; MoO_3 , 34.67%.

$[\text{MoO}_2(\text{L}^1)(\text{MeOH})]$ (**1a**): Yield: 0.085 g, 67%. Found: C, 40.80; H, 3.11; N, 9.70%. IR-ATR (cm^{-1}): 1616, 1604 ($\text{C}=\text{N}$), 1352 ($\text{C}-\text{O}_{\text{hyd}}$), 1250 ($\text{C}-\text{O}_{\text{ph}}$), 1011 ($\text{C}-\text{O}_{\text{MeOH}}$), 936, 925 ($\text{Mo}=\text{O}$), 905 ($\text{O}=\text{Mo}-\text{O}$). TG: CH_3OH , 8.00%; MoO_3 , 34.08%.

$[\text{MoO}_2(\text{L}^3)(\text{MeOH})]$ (**2a**): Yield: 0.082, 66%. Found: C, 40.31; H, 2.95; N, 9.82%. IR-ATR (cm^{-1}): 1609, 1604 ($\text{C}=\text{N}$), 1332 ($\text{C}-\text{O}_{\text{hyd}}$), 1240 ($\text{C}-\text{O}_{\text{ph}}$), 1017 ($\text{C}-\text{O}_{\text{MeOH}}$), 929, 916 ($\text{Mo}=\text{O}$), 891 ($\text{O}=\text{Mo}-\text{O}$). TG: CH_3OH , 8.20%; MoO_3 , 33.98%.

$[MoO_2(L^2)(MeOH)]$ (**3a**): Yield: 0.096 g, 77%. Found: C 40.23; H, 3.05; N, 9.95%. IR-ATR (cm^{-1}): 1619, 1611 (C=N), 1350 (C-O_{hyd}), 1256 (C-O_{ph}), 1012 (C-O_{MeOH}), 938, 912 (Mo=O), 910 (O=Mo-O). TG: CH₃OH, 7.68%; MoO₃, 33.91%.

$[MoO_2(L^4)(MeOH)]$ (**4a**): Yield: 1.14 g, 90%. Found: C 40.21; H 2.84; N 9.72%. IR-ATR (cm^{-1}): 1616, 1601 (C=N), 1342 (C-O_{hyd}), 1259 (C-O_{ph}), 1017 (C-O_{MeOH}), 936, 928 (Mo=O), 895 (O=Mo-O). TG: CH₃OH, 8.17%; MoO₃, 33.97%.

3.2. General Procedure for the Oxidation of Secondary Alcohols

Alcohol, 0.1 mL acetophenone (internal standard), and 2.5 mL acetonitrile (if added, details hereunder) were stirred together. Mo(VI) (pre)catalyst was added to the mixture. The mixture was stirred and heated to 80 °C, and the oxidant was added. The reaction was monitored by withdrawing small aliquots of the reaction mixture at a definite time interval (0, 20, 50, 90, 150, and 300 min), and analysed quantitatively by gas chromatography.

3.2.1. Carveol Oxidation

Reaction conditions: carveol (10 mmol, 1.6 mL), oxidant (20 mmol, 35% H₂O₂, 1.76 mL, or 70% TBHPaq, 2.74 mL, or TBHP in decane, $c = 5.5 \text{ mol dm}^{-3}$, 3.64 mL), 0.025 mmol of catalyst.

3.2.2. Cyclohexanol Oxidation

Protocol A

Reaction conditions: cyclohexanol (10 mmol, 1.1 mL), oxidant (20 mmol, 35% H₂O₂, 1.76 mL, or 70% TBHPaq, 2.74 mL, or TBHP in decane, $c = 5.5 \text{ mol dm}^{-3}$, 3.64 mL), 0.025 mmol of catalyst.

Protocol B

Reaction conditions: cyclohexanol (5 mmol, 0.55 mL), 35% H₂O₂ (15 mmol), 0.05 mmol of catalyst.

3.2.3. Butan-2-ol Oxidation

Without MeCN (Protocol A)

Reaction conditions: butan-2-ol (20 mmol), H₂O₂ or 70% TBHPaq (40 mmol), 0.05 mmol of catalyst.

With MeCN (Protocol B)

The same as protocol A and with 2.5 mL of MeCN.

3.3. Physical Methods

The C, H, and N mass contents were provided by the Ruđer Bošković Institute, Zagreb. Thermogravimetric analysis was performed on a Mettler TG 50 thermobalance using Al₂O₃ crucibles in an oxygen atmosphere with a flow rate of 100 cm³ min⁻¹ and heating rates of 10 K min⁻¹. IR-ATR spectra were recorded at room temperature using a Perkin Elmer Spectrum Two FTIR Spectrometer using the Attenuated Total Reflectance technique (ATR). NMR spectra were obtained on a 400 MHz Bruker Avance III HD spectrometer in dmsd-d₆.

Single-crystal X-ray diffraction data for **3·H₂O** was collected on an XtaLAB Synergy-S diffractometer with CuK α ($\lambda = 1.54184 \text{ \AA}$) radiation at 170 K. Data reduction was performed using the CrysAlis software package [29,30]. The solution, refinement, and analysis of the structures were done using the programs integrated with the WinGX [31] and OLEX2 [32] systems. All structures were solved and refined with the SHELX programme suite [33]. Structural refinement was performed on F₂ using all data. All hydrogen atoms were placed at calculated positions and treated as riding on their parent atoms. Geometrical calculations were done using PLATON [34]. Drawings of the structures were prepared using PLATON and MERCURY programs [35].

Crystal data for $3 \cdot \text{H}_2\text{O}$, $\text{C}_{13}\text{H}_{11}\text{MoN}_3\text{O}_6$ ($M = 401.19 \text{ g mol}^{-1}$): orthorhombic, space group Pbca, $a = 12.7199(2) \text{ \AA}$, $b = 12.4788(2) \text{ \AA}$, $c = 18.4185(2) \text{ \AA}$, $\alpha = \beta = \gamma = 90^\circ$, $V = 2923.55(7) \text{ \AA}^3$, $T = 170 \text{ K}$, $\mu = 7.694 \text{ mm}^{-1}$, $D_{\text{calc}} = 1.823 \text{ g/cm}^3$, 13,321 reflections collected, 3115 independent reflections, 13,321 observed reflections ($R_{\text{int}} = 0.0356$, $R_{\text{sigma}} = 0.0323$). $R = 0.0313$, $wR[I \geq 2\sigma(I)] = 0.0795$, Goodness-of-fit, $S = 1.053$ ($R = \sum | |F_o| - |F_c| | / \sum F_o$, $w = 1/[\sigma^2(F_o^2) + (g_1P)^2 + g_2P]$, where $P = (F_o^2 + 2F_c^2)/3$, $S = \sum [w(F_o^2 - F_c^2)^2 / (N_{\text{obs}} - N_{\text{param}})]^{1/2}$), No. of parameters = 213, No. of restraints = 0, $\Delta\rho_{\text{min}} = -1.15 \text{ e \AA}^{-3}$, $\Delta\rho_{\text{max}} = 0.25 \text{ e \AA}^{-3}$.

The catalytic reactions were followed by gas chromatography on an Agilent 6890A chromatograph equipped with an FID detector and a DB5-MS capillary column (30 m \times 0.32 mm \times 0.25 mm). The GC parameters were quantified using authentic samples of the reactants and products. The conversion of carveol, cyclohexanol, and butan-2-ol and the formation of cyclooctene oxide were calculated from calibration curves ($r^2 = 0.999$, 0.997, 0.999, respectively) relative to acetophenone as an internal standard.

4. Conclusions

Molybdenum(VI) complexes, mononuclear $[\text{MoO}_2(\text{L})(\text{MeOH})]$ and polynuclear $[\text{MoO}_2(\text{L})]_n$ ones, were tested as catalysts for the oxidation of secondary alcohols, carveol, cyclohexanol, and butan-2-ol, in the presence of different oxidants, H_2O_2 and THBP (in water or in decane). Carveol oxidation provided very good conversions. However, carveone yield was better with H_2O_2 and can be compared to the previously reported results. Catalytic investigation for cyclohexanol was less successful and require further optimization of reaction conditions. Although the reaction was relatively slow, selectivity towards cyclohexanone gives great potential to the tested catalytic system. In the end, butan-2-ol oxidation, with the assistance of mononuclear complexes used as catalysts, provided interesting results in terms of solvent (MeCN) addition to the investigated arrangement. For the research under these conditions, additional solvent did not show a positive effect and consequently was not needed, justifying green chemistry principles. Since the complexes with different ligand substituents showed similar results, the general conclusion was that the ligand influence on the catalysis is not significant, as well as the type of the used complex (mononuclear or polynuclear).

Supplementary Materials: The following are available online at <https://www.mdpi.com/article/10.3390/catal11080881/s1>, CCDC no: 2091707 contains the supplementary crystallographic data for this paper. These data can be obtained free of charge from The Cambridge Crystallographic Data Centre via www.ccdc.cam.ac.uk/structures.

Author Contributions: Conceptualization, J.P. and P.G.; methodology, J.M., J.P. and P.G.; validation, J.M. and M.P., formal analysis, J.M., M.P., M.M. and N.B.; investigation, J.P. and P.G.; resources, V.V., J.P. and P.G., data curation, V.V., J.P. and P.G.; writing—original draft preparation, J.M., J.P. and V.V.; writing—review and editing, P.G., J.P. and V.V.; visualization, J.M., M.P., M.M. and N.B.; supervision, P.G., J.P. and V.V.; project administration, P.G., J.P. and V.V.; funding acquisition: P.G., J.P. and V.V. All authors have read and agreed to the published version of the manuscript.

Funding: This work has been supported in part by Croatian Science Foundation under the project IP-2016-06-4221. The work of doctoral student Mirna Mandarić has been supported by the “Young researchers’ career development project—training of doctoral students” of the Croatian Science Foundation funded by the European Union from the European Social Fund.

Acknowledgments: We acknowledge the support of project CluK co-financed by the Croatian Government and the European Union through the European Regional Development Fund-Competitiveness and Cohesion Operational Programme (Grant KK.01.1.1.02.0016.). LCC CNRS and IUT Chem Dept are acknowledged for equipment for the catalysis experiments. Erasmus+ program supported the internship of J. Mihalinec and M. Pajski.

Conflicts of Interest: The authors declare no conflict of interest.

References

1. Ten Brink, G.J.; Arends, I.W.; Sheldon, R.A. Green, Catalytic Oxidation of Alcohols in Water. *Science* **2000**, *287*, 1636–1639. [[CrossRef](#)] [[PubMed](#)]
2. Chaudhuri, P.; Hess, M.; Weyhermüller, T.; Wieghardt, K. Aerobic Oxidation of Primary Alcohols by a New Mononuclear Cu(II)-Radical Catalyst. *Angew. Chem. Int. Ed.* **1999**, *38*, 1095–1098. [[CrossRef](#)]
3. Fernandes, R.R.; Lasri, J.; Guedes da Silva, M.F.C.; da Silva, J.A.L.; Frausto da Silva, J.J.R.; Pombeiro, A.J.L. Bis- and tris-pyridyl amino and imino thioether Cu and Fe complexes. Thermal and microwave-assisted peroxidative oxidations of 1-phenylethanol and cyclohexane in the presence of various N-based additives. *J. Mol. Catal. A Chem.* **2011**, *351*, 100–111. [[CrossRef](#)]
4. Guérin, B.; Fernandes, D.M.; Daran, J.-C.; Agustin, D.; Poli, R. Investigation of induction times, activity, selectivity, interface and mass transport in solvent-free epoxidation by H₂O₂ and TBHP: A study with organic salts of the [PMO₁₂O₄₀]³⁻ anion. *New J. Chem.* **2013**, *37*, 3466–3475. [[CrossRef](#)]
5. Bhatia, S.P.; Mcginty, D.; Letizia, C.S.; Api, A.M. Fragrance material review on carveol. *Food Chem. Toxicol.* **2008**, *46*, 85–87. [[CrossRef](#)]
6. Stekrova, M.; Kumar, N.; Díaz, S.F.; Mäki-Arvela, P.; Murzin, D.Y. H- and Fe-modified zeolite beta catalysts for preparation of trans-carveol from α -pinene oxide. *Catal. Today* **2015**, *241*, 237–245. [[CrossRef](#)]
7. Santos, I.; Gamelas, J.; Duarte, T.; Simoes, M.; Neves, M.; Cavaleiro, J.; Cavaleiro, A. Catalytic homogeneous oxidation of monoterpenes and cyclooctene with hydrogen peroxide in the presence of sandwich-type tungstophosphates [M₄(H₂O)₂(PW₉O₃₄)₂]_{n-}, M = Co^{II}, Mn^{II} and Fe^{III}. *J. Mol. Catal. A Chem.* **2017**, *426*, 593–599. [[CrossRef](#)]
8. Grajales, G.; Gonzáles, I.; Villa, A. Catalytic oxidative dehydrogenation of carveol to carvone over the phthalocyanine complex FePcCl₁₆ immobilized on the mesoporous silica SBA-15. *Appl. Catal. A Gen.* **2017**, *541*, 15–24. [[CrossRef](#)]
9. Cavani, F.; Ferroni, L.; Frattini, A.; Lucarelli, C.; Mazzini, A.; Raabova, K.; Alini, S.; Accorinti, P.; Babini, P. Evidence for the presence of alternative mechanisms in the oxidation of cyclohexanone to adipic acid with oxygen, catalysed by Keggin polyoxometalates. *Appl. Catal. A Gen.* **2011**, *391*, 118–124. [[CrossRef](#)]
10. Mouanni, S.; Mazari, T.; Amitouche, D.; Bendji, S.; Dermeche, L.; Roch-Marchal, C.; Rabia, C. Preparation and characterization of H_{3-2(x+y)}Mn_xCo_yPMO₁₂O₄₀ heteropolysalts. Application to adipic acid green synthesis from cyclohexanone oxidation with hydrogen peroxide. *C. R. Chim.* **2019**, *22*, 327–336. [[CrossRef](#)]
11. Hajavazzadadeh, R.; Zazi, M.K.; Mahjoub, A.R. Aliphatic alcohols oxidation with Hydrogen Peroxide in water catalyzed by supported Phosphotungstic acid (PTA) on Silica coated MgAl₂O₄ nanoparticles as a recoverable catalyst. *Int. J. Nano Dimens* **2019**, *10*, 69–77.
12. Soumini, C.; Sugunan, S.; Haridas, S. Copper oxide modified SBA-15 for the selective vapour phase dehydrogenation of cyclohexanol to cyclohexanone. *J. Porous Mater.* **2019**, *26*, 631–640. [[CrossRef](#)]
13. Maurya, M.R.; Dhaka, S.; AVECILLA, F. Oxidation of secondary alcohols by conventional and microwave-assisted methods using molybdenum complexes of ONO donor ligands. *New J. Chem.* **2015**, *39*, 2130–2139. [[CrossRef](#)]
14. Maurya, M.R.; Saini, N.; AVECILLA, F. Catalytic oxidation of secondary alcohols by molybdenum complexes derived from 4-acyl pyrazolone in presence and absence of an N-based additive: Conventional versus microwave assisted method. *Inorg. Chim. Acta* **2015**, *438*, 168–178. [[CrossRef](#)]
15. Maurya, M.R.; Neeraj, S.; AVECILLA, F. Effect of N-based additive on the optimization of liquid phase oxidation of 2 bicyclic, cyclic and aromatic alcohols catalyzed by dioxidomolybdenum(VI) 3 and oxidoperoxidomolybdenum(VI) complexes. *RSC Adv.* **2015**, *5*, 101076–101088. [[CrossRef](#)]
16. Das, S.P.; Boruah, J.J. Selective and solventless oxidation of organic sulfides and alcohols using new supported molybdenum (VI) complex in microwave and conventional methods. *Appl. Organomet. Chem.* **2020**, *34*, e5781. [[CrossRef](#)]
17. Allen, F.H. The Cambridge Structural Database, V5.30. *Acta Cryst. Sec. B Struct. Sci.* **2002**, *58*, 380–388. [[CrossRef](#)]
18. Vrdoljak, V.; Prugovečki, B.; Pulić, I.; Cigler, M.; Sviben, D.; Vuković, J.P.; Novak, P.; Matković-Čalogović, D.; Cindrić, M. Dioxidomolybdenum(VI) complexes with isoniazid-related hydrazones: Solution-based, mechanochemical and UV-light assisted deprotonation. *New J. Chem.* **2015**, *39*, 7322–7332. [[CrossRef](#)]
19. Xu, W.X.; Li, W.H. Synthesis, crystal structures, and catalytic property of dioxomolybdenum(VI) complexes with hydrazones. *Russ. J. Coord. Chem.* **2012**, *38*, 92–98. [[CrossRef](#)]
20. Vrdoljak, V.; Prugovečki, B.; Matković-Čalogović, D.; Dreos, R.; Siega, P.; Tavagnacco, C. Zigzag Chain, Square Tetra-nuclear, and Polyoxometalate-Based Inorganic–Organic Hybrid Compounds–Molybdenum vs Tungsten. *Cryst. Growth Des.* **2010**, *10*, 1373–1382. [[CrossRef](#)]
21. Bikas, R.; Lippolis, V.; Noshiranzadeh, N.; Farzaneh-Bonab, H.; Blake, A.J.; Siczek, M.; Hosseini-Monfared, H.; Lis, T. Electronic Effects of Aromatic Rings on the Catalytic Activity of Dioxidomolybdenum(VI)–Hydrazone Complexes. *Eur. J. Inorg. Chem.* **2017**, *2017*, 999–1006. [[CrossRef](#)]
22. Xu, W.-X.; Yuan, Y.-M.; Li, W.-H. Syntheses, crystal structures, and catalysis by polymeric dioxomolybdenum(VI) complexes with similar (iso)nicotinohydrazones. *J. Coord. Chem.* **2013**, *66*, 2726–2735. [[CrossRef](#)]
23. Feng, J.P.; Shi, Z. An Improved Asymmetric Synthesis of Malyngamide U and Its 2'-Epimer. *J. Org. Chem.* **2008**, *73*, 6873–6876. [[CrossRef](#)]
24. Qi, X.L.; Zhang, J.T.; Feng, J.P.; Cao, X.P. Total synthesis and absolute configuration of malyngamide W. *Org. Biomol. Chem.* **2011**, *9*, 3817–3824. [[CrossRef](#)] [[PubMed](#)]

25. Mak, K.K.W.; Lai, Y.M.; Siu, Y.H. Regiospecific Epoxidation of Carvone: A Discovery-Oriented Experiment for Understanding the Selectivity and Mechanism of Epoxidation Reactions. *J. Chem. Educ.* **2006**, *83*, 1058–1061. [[CrossRef](#)]
26. Rafiński, Z.; Ścianowski, J. Synthesis and reactions of enantiomerically pure dialkyl diselenides from the p-menthane group. *Tetrahedron Asymmetry* **2008**, *19*, 1237–1244. [[CrossRef](#)]
27. Chen, G.J.-J.; McDonald, J.W.; Newton, W.E. Synthesis of molybdenum(IV) and molybdenum(V) complexes using oxo abstraction by phosphines. Mechanistic implications. *Inorg. Chem.* **1976**, *15*, 2612–2615. [[CrossRef](#)]
28. Pisk, J.; Đilović, I.; Hrenar, T.; Cvijanović, D.; Pavlović, G.; Vrdoljak, V. Effective methods for the synthesis of hydrazones, quinazolines, and Schiff bases: Reaction monitoring using a chemometric approach. *RSC Adv.* **2020**, *10*, 38566–38577. [[CrossRef](#)]
29. CrysAlis, P.R.O. *Agilent*; Agilent Technologies Ltd.: Yarnton, Oxfordshire, UK, 2015.
30. *Oxford Diffraction, CrysAlis CCD and CrysAlis RED software, Version 1.170*; Oxford Diffraction Ltd.: Abingdon, Oxfordshire, UK, 2003.
31. Farrugia, L.J. *WinGX and ORTEP for Windows: An update*. *J. Appl. Cryst.* **2012**, *45*, 849–854. [[CrossRef](#)]
32. Dolomanov, O.V.; Bourhis, L.J.; Gildea, R.J.; Howard, J.A.K.; Puschmann, H. OLEX2: A complete structure solution, refinement and analysis program. *J. Appl. Cryst.* **2009**, *42*, 339. [[CrossRef](#)]
33. Sheldrick, G.M. Crystal structure refinement with SHELXL. *Acta Cryst. Sec. A* **2015**, *71*, 3–8. [[CrossRef](#)]
34. Spek, A.L. Structure validation in chemical crystallography. *Acta Cryst. Sec. D* **2009**, *65*, 148–155. [[CrossRef](#)]
35. Macrae, C.F.; Edgington, P.R.; McCabe, P.; Pidcock, E.; Shields, G.P.; Taylor, R.; Towler, M.; van de Streek, J.J. Mercury: Visualization and analysis of crystal structures. *Appl. Cryst.* **2006**, *39*, 453–457. [[CrossRef](#)]